MODELLING OF BUILDING CORES

Nuno Manuel Carvalho Ramilo

Instituto Superior Técnico, Department of Civil Engineering

Abstract: The aim of this work is to study the behaviour of three different ways of modelling building cores. Several items are studied and analysed by comparing the results generated by the models using a computer program (*SAP 2000*) with the ones obtained from the analytical solution.

The impact of the warping effects is also analysed by studying the longitudinal stress distribution at the core's base.

1. Introduction

Computer programs have gained a great importance in the structural analysis methods. The modelling of building structures is generally made in an easy way by using frame elements, which represent a very accurate way of simulating the beams' and the columns' behaviour. Building cores, on the other side, are a very particular case of structural modelling, since their Shear Centre is not coincident with the Centre of Gravity. Modelling the cores using frames will result in the application of the shear stress resultant forces in the wrong position. Also, frame elements do not account for the warping torsional stiffness, which represents a great part of the real torsional stiffness of open sectioned building cores.

Considering these particularities, a core will be studied in this work and three ways of modelling the core are presented and analysed. All these three ways try to simulate the real position of the core's Shear Center, as well as its real warping torsional stiffness.

2. Studied Core

The core studied in this work is presented in figure 2.1.

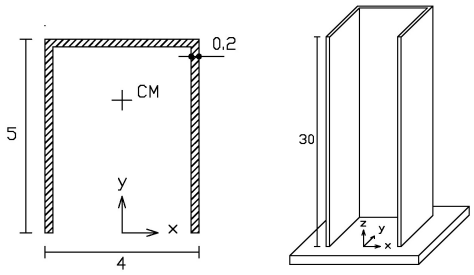

Fig. 2.1 – Core's dimensions (m)

The cross section properties used to calculate the analytical solutions presented in forward chapters are:

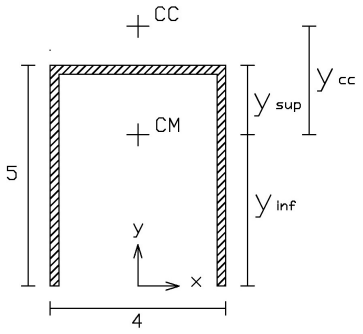

Y_{sup}	=	1,865 m
Y_{inf}	=	3,135 m
Y_{cc}	=	3,93 m
A	=	2,72 m^2
I_x	=	7,218 m^4
I_y	=	8,004 m^4
J	=	0,036 m^4
I_w	=	19,018 m^6

Fig. 2.2 – Cross sectional properties

3. Modelling

3.1. Modelling using Finite Element Method

The Finite Element Method (FEM) model was built using shell elements defined by four nodes each. The effect of the floor's slabs was simulated by using diaphragm restraints at each floor's level.

3.2. Modelling using Frame Elements

This type of modelling consists in simulating the core's behaviour with frame elements defined by two nodes with six degrees of freedom. Each wall that composes the core is simulated by a vertical frame element with the wall's cross section dimensions. The vertical frames are united by rigid horizontal frames, usually placed at each floor's level, which assure the Bernoulli's Hypothesis of the plane sections.

3.3. Modelling using Truss Panels

This type of modelling consists in simulating the core's behaviour using truss panels, such as indicated in figure 3.1.

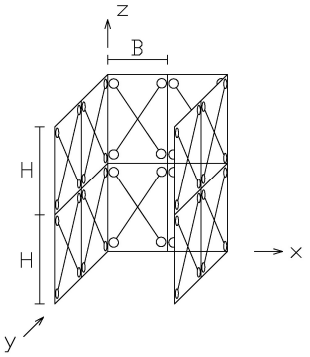

Fig. 3.1 – Part of a model using truss panels

Each panel can be built using frame elements defined by two nodes with six degrees of freedom each. The properties of those elements are such that the global behaviour of the model has to be similar to the real behaviour of the core. For that, the panel's dimensions are contained in the limits:

$$1 \leq \frac{\mathrm{H}}{\mathrm{B}} \leq 3$$

Figure 3.2 indicates a truss panel from the model.

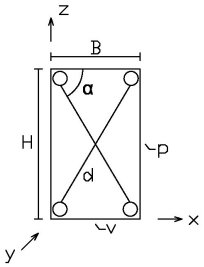

e = thickness
α = arctg H/B

Fig. 3.2 – Panel used in the model

The properties of the vertical elements (p) are:

$$I_{xp} = \frac{\frac{B}{2} \cdot e^3}{12} \qquad (3.1) \qquad I_{yp} = \frac{e \cdot \left(\frac{B}{2}\right)^3}{12} \qquad (3.2) \qquad A_p = 3A_d \qquad (3.3)$$

The properties of the horizontal elements (v) are:

$$I_{yv} = \frac{e \cdot \left(\frac{B}{2}\right)^3}{12} \qquad (3.4) \qquad I_{zv} = \frac{\frac{B}{2} \cdot e^3}{12} \qquad (3.5) \qquad \mathrm{A_V} := \frac{\mathrm{B \cdot H}}{2} \qquad (3.6)$$

Finally, the properties of the diagonals (d) are:

$$A_d = \frac{Be}{6 + 2 \cdot sen^3(\alpha)} \qquad (3.7)$$

4. Analysis of the Models

Each studied model was subject to torsional and bending loads. The behaviour of each model was compared to the analytical solutions calculated for the same load cases.

4.1. Torsion

As it is generally known, concrete elements suffer atlterations of their mechanical properties after cracking. Experimental results show that these alterations are more significant in terms of

torsional stiffness, as the Saint-Venant's torsional stiffness of these elements is severally affected.

To understand the impact of these alterations in the torsional behaviour of the cores, the torsional analysis was divided in two different cases: the first one considering Saint-Venant's torsional stiffness and the second one only considering the warping torsional stiffness.

For an inverted triangular torsional moment, distributed along the core's height, torsional rotations and the Shear Centre's position along the core's height were calculated.

For the first analysis (considering Saint-Venant's torsional stiffness), the main conclusion extracted form the results is that the frame model does not correctly simulate the core's behaviour. Figure 4.1 shows that the results can not be considered reasonable for this type of modelling.

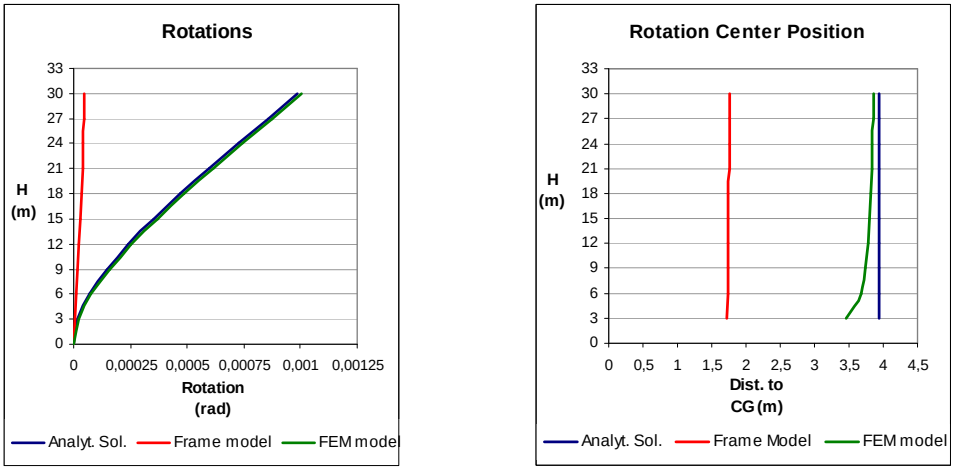

Fig. 4.1 – Results for the analysis **with** Saint-Venant's torsional stiffness

It was concluded that the rigid horizontal frames resctrict the warping effects, therefore preventing the core to rotate. Figure 4.2 indicates the warping effects on an "I" section. The longitudinal bending of the flanges requires a rotation of the web. In the frame model, the rigid frames prevent this rotation, therefore preventing the section to warp and, subsequently, to rotate.

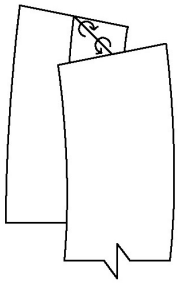

Fig. 4.2 – Warping of an "I" section

To avoid this phenomenon, the torsional stiffness of the rigid frames was not considered in the model. The results are shown in figure 4.3.

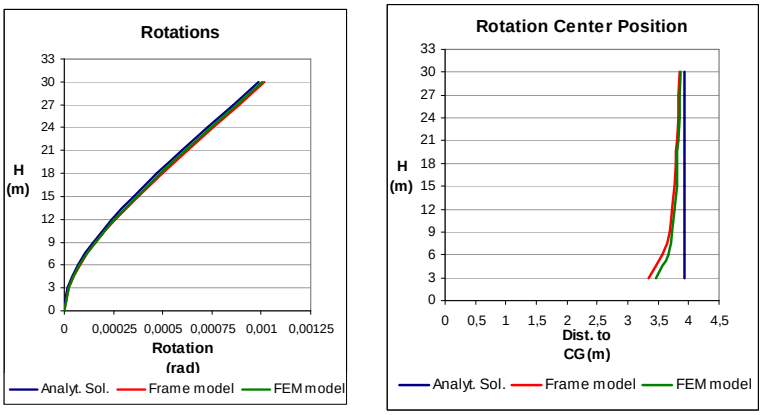

Fig. 4.3 – Modified results for the analysis **with** Saint-Venant's torsional stiffness

Also, the results for the analysis not considering Saint-Venant's torsional stiffness are presented in figure 4.4.

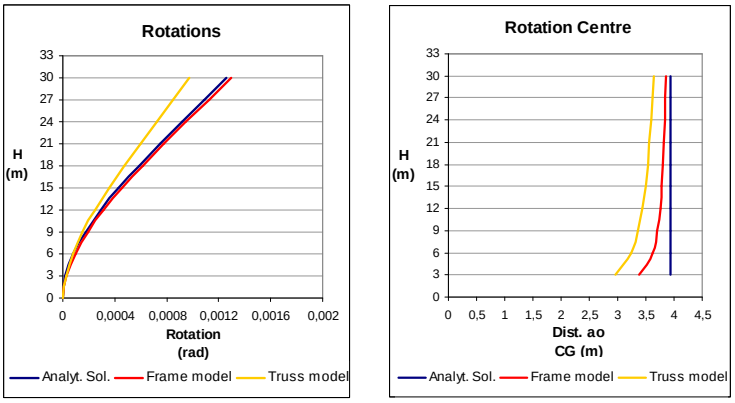

Fig. 4.4 – Results for the analysis **without** Saint-Venant's torsional stiffness

Figure 4.3 shows that with the changes made to the frame model, the results are very similar to the ones calculated analytically. The problem detected in figure 4.2 can be easily solved by not considering the torsional stiffness of the rigid frames. Also, the results obtained form the FEM model seem to be quite accurate, mainly in terms of rotations.

Figure 4.4 indicates that the results obtained from the Truss Model are not so accurate as the ones generated using other models. Despite these differences, in practical terms, the results can be considered satisfactory.

The analysis of the two figures showed that not considering Saint-Venant's torsional stiffness resulted in an increase of the rotations at the top of about 30%. This value is, though, strongly dependent of the cross section's properties. It is also important to notice that the frame model

could simulate successfully the impact of not considering Saint-Venant's torsional stiffness generating very similar results to the analytical ones in both analysed cases.

4.2. Bending

Bending analysis was made separately for both "x" (web) and "y" (flanges) directions. To avoid torsional rotations when subjecting the core to bending in "x" direction, rotations around "z" axis were restrained. This analysis was made subjecting the core to an inverted triangular distributed load.

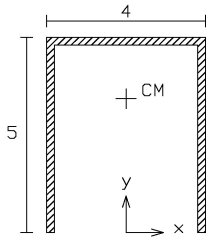

Fig. 4.5 – Directions considered in the analysis

The results obtained for each bending direction are presented in figure 4.6.

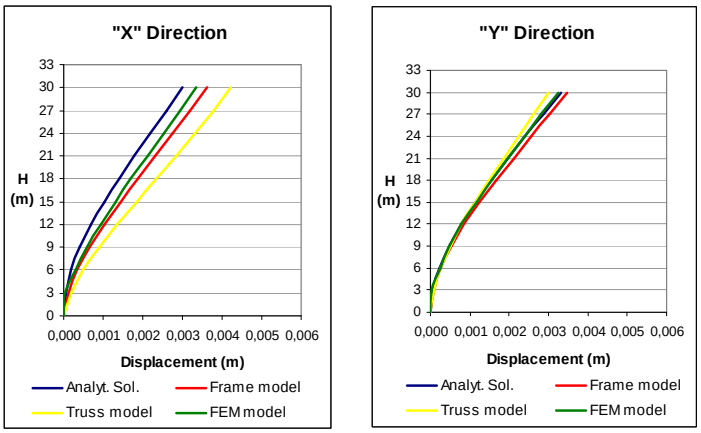

Fig. 4.6 – Results for the bending analysis – directions "x" and "y"

The presented results show that all the models simulate more effectively the core's bending behaviour in "y" direction. The differences for the analytical solution obtained for bending in "x" direction may be related to shear lag phenomena. The analytical solution obtained is based on Bernoulli's hypothesis of the plane sections. However, this hypothesis is not valid for both FEM and Truss models, therefore, this fact may origin the differences observed.

The changes made to the Frame model, can also explain the differences observed. These changes are expected to cause a loss of efficiency in the connection between the vertical frames. In fact, for bending in "x" direction, figure 4.7 indicates that the Bernoulli's Hypothesis is no longer verified. This fact may be responsible for the differences observed. On the other side,

figure 4.8 shows that for bending in “y” direction, Bernoulli’s Hypothesis is still verified, therefore the results obtained are very similar to the ones calculated analytically.

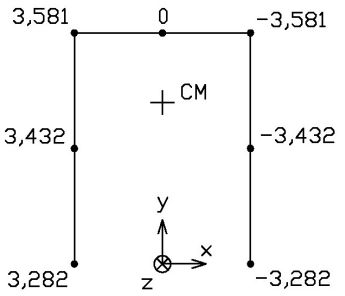

Fig. 4.7 – Bending in “x” direction – Vertical displacements at the top (x10^{-4}m)

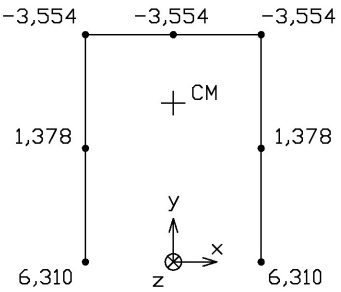

Fig. 4.8 – Bending in “y” direction – Vertical displacements at the top (x10^{-4}m)

5. Longitudinal Stress Analysis

5.1. Longitudinal Stress Diagrams at the Base

To evaluate the capacity of each model to simulate the real elastic longitudinal stress distribution at the core’s base, each model was subject to distributed loads in both “x” and “y” directions, as well as a vertical load. The corresponding forces at the core’s base are:

Mx = 9000 kNm My = 9000 kNm T = 930 kNm N = -5740 kN

To observe the impact of the warping effects, the analytical longitudinal stress distribution at the base was calculated with and without the longitudinal stress due to the warping effects.

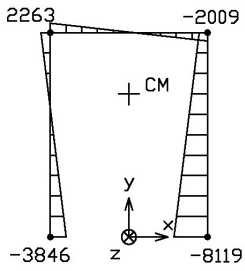

a) Without warping effects

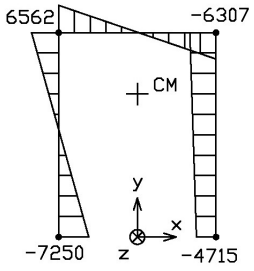

b) With warping effects

Fig. 5.1 - Longitudinal stress distribution at the base: analytical solution

For the same loadcases, the stress diagrams obtained from both FEM and Frame models were:

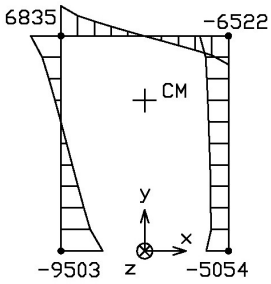

a) FEM model

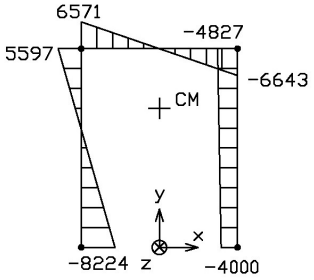

b) Frame model

Fig. 5.2 - Longitudinal stress distribution at the base

Figure 5.1 shows that the warping effects can significantly change the values of the longitudinal stress distribution. The tension values for the solution with warping effects are three times higher than the ones calculated ignoring those effects. Also the calculated values for the compressed areas of the section have significantly changed.

On the other side, figure 5.2 shows that both models can successfully reproduce the analytical stress distribution presented in figure 5.1 b). Despite the differences observed, the stress diagrams present a similar shape and the observed values could successfully simulate the analytical ones, particularly in the presence of warping effects.

5.2. Longitudinal Reinforcement

To account for the warping effects, an easy way of calculating the longitudinal reinforcement steel area is proposed and applied. The results obtained form each model are compared to a solution obtained using a computer program for composed oblique bending calculation.

Figure 5.3 indicates the process used to calculate the steel area using both FEM and Frame models. The figure represents the stress distribution in a core's general wall.

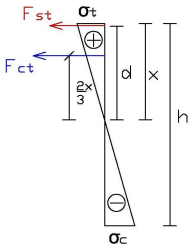

F_{ct} – Concrete tension resultant forces

F_{st} – Steel tension resultant forces

$$Fct = \frac{\sigma_t \cdot x}{2} \cdot e \qquad (5.1)$$

$$Fst = A_s \cdot f_{yd} \qquad (5.2)$$

Fig. 5.3– Diagram used to calculate the longitudinal steel area

$$Fct \cdot \frac{2}{3} x = Fst \cdot d \qquad (5.3)$$

$$Fst = \frac{\sigma_t \cdot x^2 \cdot e}{3d} \qquad (5.4)$$

The longitudinal steel area to adopt is given by the expression:

$$A_s = \frac{Fst}{f_{yd}} \tag{5.5}$$

For the Truss model, the reinforcement steel area was calculated using the values of the vertical force at each node of the studied section of the model – in this case, the base section.

The steel area value is, therefore, calculated by expression (5.6). "F_v" represents the vertical force at each node.

$$A_s = \frac{F_v}{f_{yd}} \tag{5.7}$$

The steel reinforcement area obtained from the computer program is presented in figure 5.4. The solutions obtained from each model, using the processes proposed in this chapter, are presented in figure 5.5.

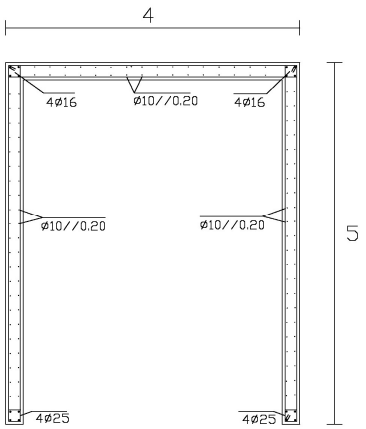

Fig.5.4 – Solution obtained from the computer program (without warping effects)

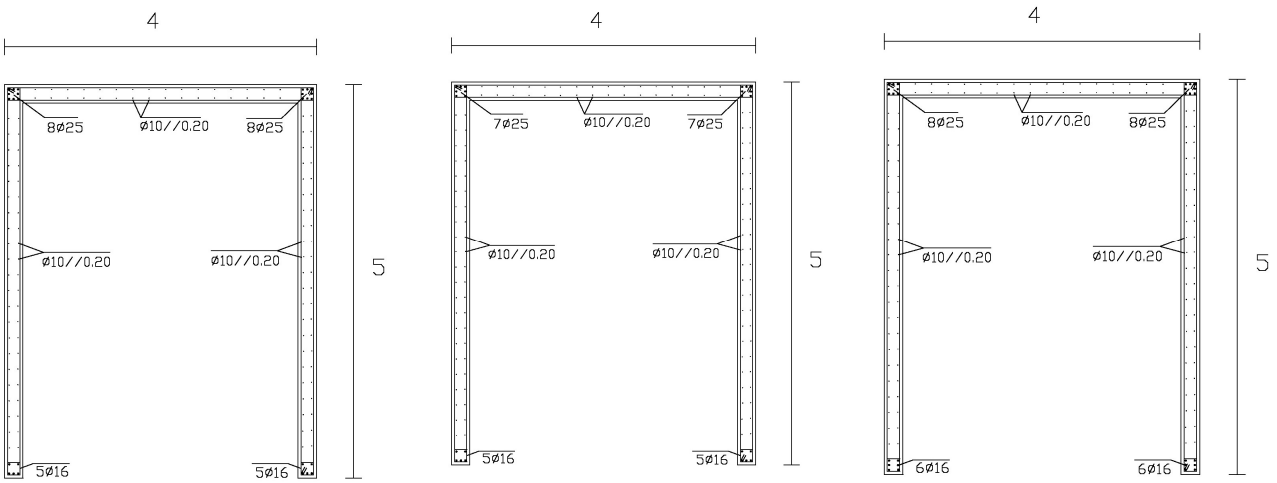

a) FEM Model b) Frame Model c) Truss Model

Fig.5.5 - Solutions obtained form the models

Although the results obtained from each model are very similar among each other, all of them are quite different from the one obtained from the computer program. These results are consistent with the ones presented in chapter 5.1 and indicate that the warping effects can effectively change the value and the distribution of the longitudinal steel reinforcement at the core's base.

6. Conclusions

The main conclusions extracted from this work are:

- The Frame model can only correctly simulate the core's behaviour if the torsional stiffness of the rigid frames is not considered. Otherwise, the model cannot simulate correctly the torsional behaviour of the core.

- Considering this alteration to the Frame model, all the models could successfully simulate the core's behaviour. The differences observed can be considered acceptable when compared to the approximations made in the evaluation of the seismic actions.

- The warping effects can effectively change the values and the distribution of the longitudinal stress at the core's base. All the models could simulate successfully these alterations.

- The results obtained using the proposed methods to calculate the longitudinal steel reinforcement area were very similar for all the models. These results were significantly different from the ones generated by a computer program that ignored the warping effects.

7. References

Lopes, M., “Comportamento de Núcleos de Edifícios”; Master Thesis; Departamento de Engenharia Civil, Instituto Superior Técnico, Lisboa, 1987

Branco, F. A., “Pontes Mistas em Caixão”, PhD Thesis, Departamento de Engenharia Civil, Instituto Superior Técnico, Lisboa, 1984

Borges Pires, E., “Resistência de Materiais”, Instituto Superior Técnico, 1987

Reis, A.J., “Folhas da Disciplina de Pontes” Instituto Superior Técnico, Revisão 2006

Eurocode 8, “Design of Structures for Earthquake Resistance”, CEN, Brussels, 2004

Gomes, T. C., “Estudo Comparativo de Processos Contínuos para a Análise de Núcleos Estruturais Submetidos à Torção”, Master Thesis, Universidade Estadual de Campinas, 1999

Parreira, P., Conversation with the Author, Lisboa, 2009-07-16

Pinto, F., “Modelação e Dimensionamento de Núcleos de Betão Armado em Edifícios Sujeitos à Acção Sísmica”, Master Thesis, Departamento de Engenharia Civil, Faculdade de Engenharia da Universidade do Porto, Porto, 1998

site www.imc.ep.usp.br: Projecto FAPESP – Tecnologia Educacional – Ensino de Engenharia de Estruturas

Gomes, A., Vinagre, J., “Betão Armado e Pré-Esforçado I: Tabelas de Cálculo”, Instituto Superior Técnico, Setembro de 1997

Smaniotto, A., “Dimensionamento e Detalhamento Automático de Pilares Rectangulares Submetidos à Flexão Composta”, Master Thesis, Universidade Federal de Santa Catarina

Computers and Structures, Inc., [2007] “CSI Analysis Reference Manual for SAP 2000”, Berkeley, CA, USA, April 2007.